An experimental investigation of the stability of peeling for adhesive tapes

C. Kovalchick, A. Molinari, G. Ravichandran

An experimental investigation of the stability of peeling for adhesive tapes

C. Kovalchick [a], A. Molinari [b], G. Ravichandran [a,*]

[a] *Graduate Aerospace Laboratories, California Institute of Technology, Pasadena, CA 91125, USA*
[b] *Laboratoire d'Etude des Microstructures et de Mécanique des Matériaux, Université de Lorraine, Ile du Saulcy, 57045 Metz Cedex 01, France*

A fundamental question of interest in peeling is the stability of the debonding process. A new experimental configuration has been developed to investigate the stability of the peel-ing process of elastic tapes. The experimental method allows for independent variation of the applied load and stiffness of the system. The role of various parameters including the stiffness of the loading system and geometry of the tape on the stability of peeling is inves-tigated. The change in stiffness can be tuned to trigger or delay the onset of instability. Theoretical stability criteria are used to develop insights into the role of various experimentally varied parameters on the stability of the peeling process.

1. Introduction

The applications of peeling and adhesion are widespread in both engineering and biology. A specific problem that has captivated the attention of a diverse group of scientists during the last decade is the enhancement of the adhesive strength by studying analogous behavior in nature such as the gecko. More specifically, investigations focused on naturally-occurring reversible adhesion in biological systems can be applied to the development of engineered adhesive systems, which have a wide range of applications including pressure sensitive tapes (Benedek and Feldstein, 2008), biomedical devices (Bundy et al., 2000), microelectronic storage and packaging (Harris and Rubel, 2008), and surgical robotics (Balicki et al., 2010).

A fundamental question of interest in peeling is the stability of this process. The role of various parameters including adhesion energy, compliance of the loading system, and geometry of the film on the stability of peeling are of interest. Recent studies have focused on understanding the role of stability in the gecko adhesion problem (Autumn et al., 2006; Tian et al., 2006; Yao and Gao, 2006), particularly with regard to the force distribution in the contact of the gecko's foot to a surface and the detachment of setae (Autumn et al., 2006; Cheng et al., 2011).

The investigation of the stability of peeling can be viewed as an application of concepts in fracture mechanics (Hutchinson, 1979; Hutchinson and Paris, 1979) to the peel test but has received relatively little attention. This study aims to investigate the stability of peeling including the role of compliance of the loading system. Experiments are conducted to monitor the position of the peel tip in an inextensible adhesive tape over time subject to a constant vertical load applied at the tape extremity while the width of the tape is decreased as a function of the tape length. In addition to examining the effect of the applied load and the change in width on the stability of the debonding process, the stiffness of the loading system is varied using an elastic spring. This change in stiffness in a direction parallel to the substrate also affects the peel tip velocity, and can be tuned to trigger or delay the onset of instability. Experimental observations are interpreted

* Corresponding author. Tel.: +1 (626) 395 4525; fax: +1 (626) 449 2677.
E-mail address: ravi@caltech.edu (G. Ravichandran).

within a theoretical framework for the stability of the debonding of an inextensible tape from a rigid substrate.

A brief summary of results from the theory of stability for peeling (Molinari and Ravichandran, 2013) is presented in Section 2, which provides the background to interpret the experimental results presented later. The materials and experimental methods employed in this study are described in Section 3. A new method for altering the system compliance is introduced and is used to investigate its effect on stability of peeling. Results of the investigation are presented in Section 4 and are discussed in light of the theoretical model outlined in Section 2. The conclusions for the study are presented in Section 5.

2. Theory

Consider the peeling of an inextensible tape from a rigid substrate. The tape is subjected to a vertical force (F_{perp}) through a dead load (weight) and a horizontal force (F_{par}) through a compliant spring loading mechanism that is parallel to the tape adhered to the substrate. The loading arrangement, forces acting on the tape and the geometry of the tape are shown schematically in Fig. 1(a–c). F_{par} and F_{perp} represent the forces parallel and perpendicular to the substrate, respectively (Fig. 1(b)) resulting in the net force F acting along the tape. The loading arrangement in Fig. 1(a) is analogous to the adhesion system of a gecko, where the vertical force (F_{perp}) can be interpreted as the weight of the gecko while the horizontal force (F_{par}) is due to the compliant mechanism of the muscles in the legs. The vertical force F_{perp} in this configuration will remain constant during experiments to be discussed here, to ensure the peeling condition.

The resultant force, F acting along the backing of the tape provides the driving force for peeling the tape from the substrate,

$$F = \frac{F_{perp}}{\sin\theta}, \tag{1}$$

where θ is the current peel angle.

The peel tip position is defined as a, with $a = 0$ corresponding to the initial tip position at the onset of peeling. The peel angle θ evolves with the advance of the peel front. If the tape is assumed to be inextensible and the tape extremity is constrained to move vertically (either by vertically guided dead weight, F_{perp} or displaced vertically), the peel angle decreases from an initial peel angle θ_o according to the following relationship:

$$\theta = \cos^{-1}\left(\frac{l_o\cos\theta_o + a}{l_o + a}\right), \tag{2}$$

where l_o and $l = (l_o + a)$ are the initial and current lengths of the peel arm, respectively.

In the present analysis, the tape is assumed to be inextensible, and the debonding or adhesion energy is assumed to be a material constant, which is independent of position, peel angle, and peel velocity. For constant adhesion energy γ and inextensible tape, Rivlin (1944) derived the expression for the peel force per unit width,

$$P_f = \frac{\gamma}{1-\cos\theta} \tag{3}$$

and the adhesion energy can be expressed as,

$$\gamma = P_f(1-\cos\theta). \tag{4}$$

Eq. (3) can be used to plot the peel force as a function of the peel angle and will be referred to hereafter as the Rivlin

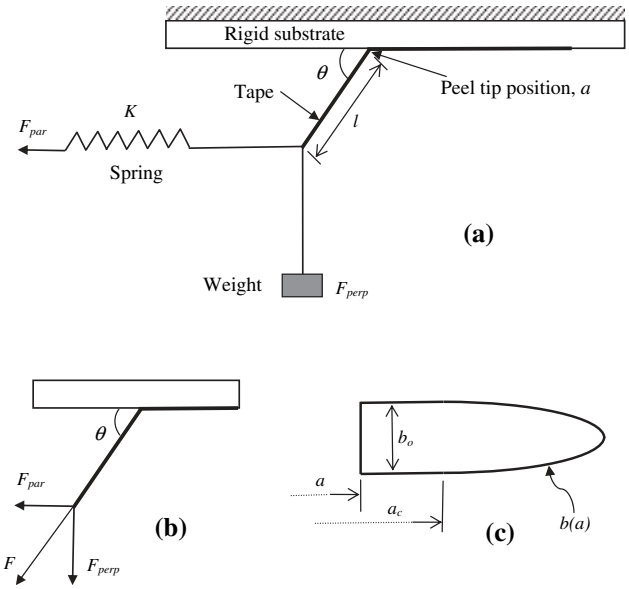

Fig. 1. (a) Schematic of the peeling configuration for studying stability under combined loading with varying system stiffness provided by the horizontal spring. The vertical force F_{perp} is not necessarily confined to fixed plane perpendicular to the substrate during peeling. When required to confine the load F_{perp} to a fixed plane, a vertical guide is used. (b) Forces acting on the tape that is being peeled: F_{par} and F_{perp} are the forces in directions parallel and perpendicular to the tape adhered to the substrate, respectively. F is the resultant peel force acting along the backing of the tape. (c) Geometry of the tape adhered to the substrate: the tape width has a constant value, b_o, which may change to a variable width $b(a)$ when the peel tip reaches the position, $a = a_c$.

curve (Fig. 2), which corresponds to the material resistance of the adhesive interface to peeling the tape from the rigid substrate.

Analogous to crack propagation in fracture mechanics, peeling will occur when the energy available for debonding (G) is equal to the adhesion energy (γb)

$$(G - \gamma b) = 0, \quad \text{or} \quad G - F(1 - \cos\theta) = 0, \tag{5a, b}$$

where b is the width of the tape, which may vary with the position of the peel tip. Equation (4a) relates the debonding or adhesion energy γ to the peel force per unit width P_f and peeling proceeds when the force along the tape backing is equal to $F = bP_f$.

In Fig. 2, the solid curve represents the resistance to peeling, $F = bP_f$, given by the Rivlin expression (Eq. (3)), while the dashed curve represents the driving force for debonding due to the applied load (Eq. (1)). The values of the adhesion energy $\gamma = 30$ N/m and constant width, $b = 48$ mm are used in plotting the Rivlin curve, which correspond to the values for Scotch™ Sure Start Shipping Packaging Tape (3M, Minneapolis, MN) (Kovalchick, 2011).

To best understand the utility of Fig. 2, consider the case where a constant load F_{perp} (2.45 N (250 g)) guided vertically is applied to a tape of constant width with an initial peel angle (θ_o) of 90°. The initial applied force corresponds to the right extremity of the dashed curve. At this point, the driving force curve is above the Rivlin curve, designated as region C on the plot. This region corresponds to the case where the driving force $\frac{G}{b} = \frac{F_{perp}(1-\cos\theta)}{b\sin\theta}$ (energy release rate divided by width of the tape) is larger than the adhesion energy, γ. Then, debonding in this region is unstable and the tape will peel off, advancing the tip position, a. As the tape is peeled, the angle will decrease as suggested by Eq. (2). Following the driving force curve, this curve will intersect theRivlin curve at an angle of $\theta = 68°$. At this intersection (B), the tape will no longer debond and the propagating tip will arrest reaching equilibrium. For the tape to debond further, a larger force must be applied, so as to shift the driving force curve upwards.

The stability of peeling of elastic tapes and its dependence on the system stiffness is analogous to the stability of crack in a fracture specimen and its dependence on machine compliance (Hutchinson, 1979; Hutchinson and Paris, 1979). The peeling (debonding) is unstable if,

$$\frac{d(G - \gamma b)}{da} > 0, \tag{6}$$

while the peeling (debonding) is stable if,

$$\frac{d(G - \gamma b)}{da} < 0. \tag{7}$$

Assuming that the peeling criterion (Eq. (5)) is met, the following expression serves as the basis for examining the stability in peeling of inextensible tapes from a rigid substrate (Molinari and Ravichandran, 2013),

$$\frac{d(G - \gamma b)}{da} = \frac{-bP_f(1-\cos\theta)^2 - b'P_f(1-\cos\theta)\left(l\sin^2\theta + \frac{bP_f}{K}\right)}{l\sin^2\theta + \frac{bP_f}{K}}, \tag{8}$$

where b' is the derivative of the tape width with respect to peel tip position (i.e., db/da) and K is the stiffness of the loading system in the direction parallel to the substrate.

Stability results have been obtained by Molinari and Ravichandran (2013) for extensible and inextensible tapes and for debonding energy γ being rate independent but depending upon peel angle and position. The stability of the debonding process was checked by examining, at the critical condition $G = \gamma b$, whether debonding could proceed without moving the left extremity of the spring horizontally (see Fig. 1a). Some details about the derivation of Eq. (8) are provided here. In the present paper, it is assumed that the tape is inextensible and that the debonding energy is constant. Considering that the applied weight F_{perp} is fixed, it follows from Eqs. (1) and (4) that $dG = F_{perp}\frac{d\theta}{1+\cos\theta}$, where $d\theta$ is the variation of the peel angle

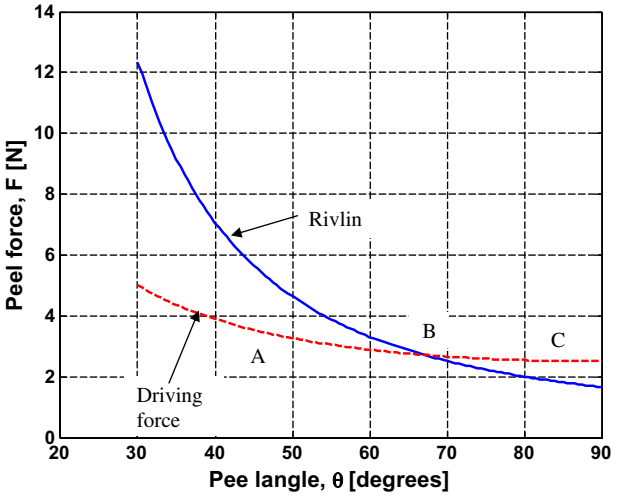

Fig. 2. Peel force, F as a function of the peel angle, θ. The solid curve represents the resistance to peeling, $F = bP_f = \frac{b\gamma}{1-\cos\theta}$, given by the Rivlin relation, Eq. (3), while the dashed curve represents the driving force for debonding, $F = \frac{F_{perp}}{\sin\theta}$ due to the applied vertical load, F_{perp}.

resulting from the incremental advance of debonding, *da*. It was shown by Molinari and Ravichandran (2013) that these increments are related by:

$$d\theta = \frac{\cos\theta - 1}{\frac{F_{perp}}{K(\sin\theta)^2} + l\sin\theta} da \tag{9}$$

Finally, Eq. (8) is obtained by combining these results and by considering the relationship, $F_{perp} = P_f b \sin\theta$.

The energy release rate represents the energy in the system available for debonding provided externally through the applied loading, *F*, and internally by the elastic energy stored in the spring. Similar to the analogous results in fracture mechanics (Hutchinson, 1979; Hutchinson and Paris, 1979), the stability criterion (Eq. (8)) is influenced by the geometry of the tape that is being peeled, i.e.,*l*, *b* and θ.

For the case of a tape with constant width ($b' = 0$), the expression in Eq. (8) can be simplified:

$$\frac{d(G-\gamma b)}{da} = \frac{-bP_f(1-\cos\theta)^2}{l\sin^2\theta + \frac{bP_f}{K}}. \tag{10}$$

For this case, debonding is always stable since the right hand side is negative and thus achieving the condition in Eq. (7).

Now consider the case where the tape width decreases as the peel tip advances, i.e., $b' < 0$. Debonding in this case is stable if, $bP_f(1-\cos\theta)^2 + b'P_f(1-\cos\theta)\left(l\sin^2\theta + \frac{bP_f}{K}\right) > 0$, or simplified in a more convenient form,

$$b' > -\frac{b}{l}\frac{(1-\cos\theta)}{\left(\sin^2\theta + \frac{bP_f}{Kl}\right)}. \tag{11}$$

These results show that as the spring stiffness (*K*) is decreased, the system moves towards the unstable state. Thus, by manipulating the stiffness, the system can be moved between stable and unstable peeling. Important observations can be made by examining the two extreme cases for the stiffness of the spring: $K = \infty$ (rigid) and $K = 0$ (compliant). Note that $K = \infty$ corresponds to the case where the dead weight (F_{perp}) is guided vertically (no horizontal displacement of the tape extremity) or displaced vertically at the tape extremity.

For $K = \infty$, consider two separate cases denoted by #1 and #2, in which the same initial values are imposed for the initial width, peel arm length and peel angle, b_o, l_o and θ_o, respectively. The difference will be in the relation for the change of width in Eq. (11) such that for #1:

$$b' > -\frac{b_o}{l_o(1+\cos\theta_o)}, \tag{12}$$

and for #2:

$$b' < -\frac{b_o}{l_o(1+\cos\theta_o)}. \tag{13}$$

For case #1, the debonding of the tape is initially stable. However, for case #2, the debonding is initially unstable. Thus, by tuning the geometrical parameters *b*, l_o and θ_o with respect to the value of b', instability in peeling can be triggered or avoided.

Finally, considering the other extreme of stiffness that of an infinitely soft (compliant) loading mechanism where $K = 0$, Eq. (8) can be expressed as,

$$\frac{d(G-\gamma b)}{da} = -b'P_f(1-\cos\theta). \tag{14}$$

Thus, in this case, debonding is unstable for $b' < 0$ and stable for $b' > 0$.

The effect of various parameters such as varying tape width (b') and the stiffness of the loading system (*K*) on the stability of the peeling process will be examined experimentally in the following sections.

3. Experimental

An experimental setup has been developed for conducting peel tests of an adhesive tape attached to a rigid glass substrate. The tape is subjected to a weight in the direction perpendicular to the tape (F_{perp}), with loading parallel to the substrate (F_{par}) applied using a compliant spring system with a known stiffness (*K*). The combination of applied loading (F_{perp} and F_{par} in Fig. 1(b)) can be varied over a wide range.

The newly developed experimental setup for studying stability of peeling is shown pictorially in Fig. 3 and incorporates all the loading elements shown schematically in Fig. 1(a). The tape is adhered to the underside of a glass substrate, held between two acrylic glass plates (12.7 mm (0.5″) thick) each with a 127 mm (5″) radius cut-out, which enables the imaging of the peel tip. Two pieces of Delrin held together by two screws, are used as a grip to clamp the end of the tape. A rectangular receptacle is tied to the ends of the screws of the grip with 89 N (20 lbf) fishing wire. Small spherical beads each weighing 2.94 mN (0.3 g) are added into the receptacle to achieve the desired weight.

Experiments are conducted using Scotch™ 3450S-RD Sure Start Shipping Packaging Tape (3M, Minneapolis, MN), which has a width $b = 48$ mm (1.88″) and thickness $t = 66$ μm (2.6 mil). This specific adhesive tape is chosen because of its large width, which is useful in conducting stability experiments where the width changes as a function of position. The backing material of this tape is observed to behave in a linearly elastic manner, with the Young's modulus obtained independently through uniaxial tension tests ($E = 1.6$ GPa). The tape can be considered to be inextensible since the maximum strain computed for the experiments is less than 0.25%. Prior to the experiment in all cases, the glass surface is cleaned with acetone, followed by wiping with isopropanol, and left to dry. The adhesive tape is applied to the glass surface with a roller to achieve uniform adhesion to the substrate. Experiments are conducted after the adhesive is left to rest for 20 min prior to start of the experiment. Constant peel rate tests were conducted to determine the adhesion energy (γ), which was determined to be 30 N/m for the tape attached to glass substrate peeled at 10 μm/s (Kovalchick, 2011).

Two distinct loadings are considered in this investigation: (I) loading perpendicular to the substrate (F_{perp}) using a vertically guided weight, with the horizontal spring

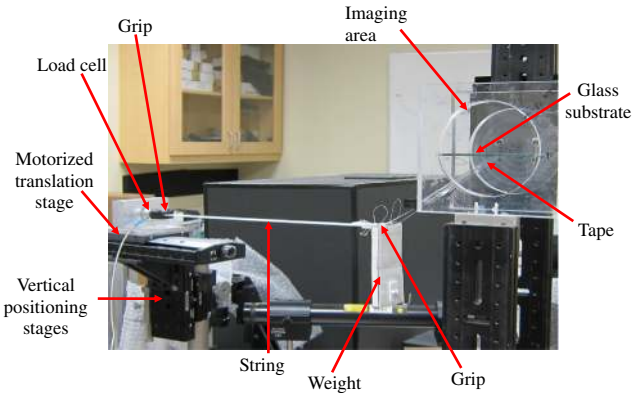

Fig. 3. Variable stiffness experimental setup, which incorporates a string with known stiffness parallel to the substrate attached to the tape, which applies loading parallel to the substrate (F_{par}) and the weight, which applies loading perpendicular to the substrate (F_{perp}).

(Fig. 1(a)) being absent in this configuration. The guide perpendicular to the substrate is formed using a vertically mounted thin aluminum plate attached to a 304 mm (12″) optical rail. As the load descends vertically in the guide while the tape debonds from the substrate during the experiment, the peel angle θ changes continuously (Eq. (2)). This corresponds to a loading system with infinite stiffness ($K = \infty$) parallel to the substrate. An alternate approach to using the vertical guide is to use an infinitely stiff spring attached horizontally to the tape. (II) The load perpendicular to the substrate (F_{perp}) is applied using the weight attached to the tape and the horizontal loading parallel to the substrate (F_{par}) is applied using an elastic spring with known stiffness K. In this configuration, the perpendicular load F_{perp} remains constant during the test, so that the peeling condition given in Eq. (5) is fulfilled by adjusting the force F_{par} during the peeling process.

To implement compliance control in the horizontal direction, an elastic string of rectangular cross-section with a thickness (t_s) of 1 mm (Elastic strap, Michael's, Irving, TX) is woven through a slot in the weight receptacle and clamped at the end with a fastener. Variable lengths and widths of the elastic string are used to alter the stiffness, K and thus the force parallel to the substrate, F_{par}. The string is clamped at the other end by a similar Delrin grip to the one used to hold the extremity of the tape. The grip is attached to a 500 g load cell (ALD-MINI-UTC-M, AL Design, Inc., Buffalo, NY), which is attached to an aluminum T bracket and fixed to a motorized translation stage (M-410.CG, Physik Instrumente, Irvine, CA). The stage has a total travel range of 100 mm, a maximum velocity of 1 mm/s, and displacement resolution of 100 nm. The stage is mounted on an optical T bracket, which is attached to a linear translation stage mounted vertically on an optical post. The optical post is mounted to a separate linear translation stage fixed to an optical table.

The load from the load cell is monitored *in situ* with a digimeter (MD-40, Newport, Irvine, CA), configured to show the output force from the load cell. The initial parallel force, F_{par0}, is determined by setting the tension in the string and observing the value through the digimeter. The parallel force F_{par} is decreased during a test by moving the stage towards the right (i.e., towards the tape's extremity), which relaxes the tension in the string. Data is acquired at a rate of 5 samples per second for the duration of an experiment from the load cell through a virtual instrument created in Labview (DAQM02, National Instruments, Austin, TX). The test times are typically on the order of one hour (3600 s). As the applied weight (F_{perp}) descends when the tape is peeled, the height of the motorized translation stage is manually adjusted in small increments to keep the string parallel to the substrate.

The stiffness (K) of the elastic string can be changed by varying its geometry to alter the parallel force F_{par}. Consider an elastic string attached to the extremity of the tape to apply the parallel force F_{par}. The stiffness K is defined as,

$$K = \frac{F_{par}}{\delta}, \tag{15}$$

where F_{par} is the force and δ is the resultant string elongation. By relating Eq. (14) to the geometry and material properties,

$$K = \frac{Ewt_s}{L_s}, \tag{16}$$

where E is the Young's modulus of the string material and w, t_s, and L_s are the width, thickness, and length, respectively, of the elastic string of rectangular cross section. If the length and thickness of the string remain constant, the stiffness K increases as the tape width is increased. Note that an infinitely compliant loading system ($K = 0$) can be achieved by employing a very long string ($L_s \to \infty$).

The position of the peel tip of the tape is continuously monitored and imaged during the experiments. The tip position, a, is defined as the contact point between the tape and the glass substrate. The tip is imaged with a 2-megapixel monochromatic digital CCD camera (UP-2000CL B/W, Uniqvision, Santa Clara, CA; not shown in Fig. 3). During the experiments, one image is acquired every 5 s for the duration of the test. Fig. 4 shows a sample image of the tape debonding from the glass substrate during a constant vertical force (F_{perp}) experiment. To track the tip position, a, over time, all of the images from a given test are loaded sequentially in Matlab (Mathworks, Natick, MA) and the tip position is located manually by examining each image. The selected tip position is stored for each image and sub-

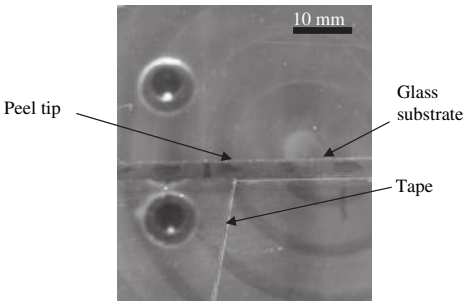

Fig. 4. Image of the tape being peeled from the substrate to locate its peel tip position, a, as acquired with a CCD camera in a peeling experiment.

sequently tracked over time. Using this imaging technique, the tip position of the tape as a function of time is constructed.

The experiments utilize tapes of either constant width or tapes that go from constant to variable width (Fig. 1(c)). The variable width tapes have a region of constant width followed by a section where the width changed as a linear function of the tape position,

$$b = b_o - \frac{2}{5}(a - a_c) \text{ for } 0 < (a - a_c) < \frac{5}{2}b_o, \tag{17}$$

where a is the current peel tip position in the region of varying width and a_c is the position on the tape where the width begins to change.

Three different types of experiments are conducted with the newly developed experimental configuration shown in Fig. 3. In addition, displacement-controlled experiments are also performed to demonstrate the tuning of stability through geometrical parameters.

In the first set of experiments, a tape of constant width followed by variable width (Eq. (17)) is subjected only to the vertically guided force (F_{perp}). The tape is subjected to successive application of two separate prescribed vertical loads and the effect of the change in tape width on stability of peeling is investigated. This corresponds to the case where $K = \infty$ and is used to examine this limiting value of K on the stability of peeling for a variable tape width ($b' < 0$). The stability/instability conditions as predicted by Eqs. (12) and (13) are validated with this set of experiments.

The second set of experiments is conducted for a tape of constant width under combined loading of the weight (F_{perp}) and the horizontal force (F_{par}) applied through a compliant string. Two different strings with different widths are used for varying combinations of vertical (F_{perp}) and the initial parallel (F_{par0}) force which produce the same initial resultant peel force F (Eq. (1)). The tape is initially set at a shallow initial peel angle to change the equilibrium condition quickly along the driving force curve (Fig. 2) to propagate peeling. The stage is set to move at a constant velocity for a prescribed duration of the experiment, slowly releasing the tension in the string and thus decreasing F_{par}. The goal is to investigate how altering the parallel and perpendicular force components affect the tip velocity and the stability of peeling and provides a direct validation of the prediction of the dependence of stability on the stiffness K as given by Eq. (8).

In the third set of experiments, the values of F_{perp} and F_{par0} are prescribed and the width of the tape is varied (Eq. (17)). F_{par0} is the initial value of the force in the horizontal string and a string of same width (w) (stiffness, K) is used in all experiments. The horizontal loading stage is moved so as to decrease the tension in the string for varying amounts of time and then stopped. By stopping the stage at different times, the parallel force component F_{par} will be different and its effect on the stability, particularly in the variable width portion of the tape, can be examined. This set of experiments is used to validate the prediction given by Eq. (11).

In the second and third set of experiments, as the parallel force component is reduced by the motion of the motorized stage while holding the vertical force constant, the change in angle results in satisfying the peeling criterion in Eq. (5), i.e., $G - \gamma b = 0$, thus sustaining peeling.

The peel arm length (l) has a direct effect on the stability of peeling as seen from Eqs. (8), (10) and (11). Even in the case where $K = \infty$, the initial peel arm length (l_o) is an important parameter in determining the stability of peeling (Eqs. (12) and (13)). The role of the peel arm length has not been examined explicitly in the present study but has been accounted for while examining stability using the experimental data from the experiments.

4. Results and discussion

4.1. Prescribed vertical load (F_{perp})

The experimental setup shown in Fig. 1 is used without the horizontal string, while the weight (F_{perp}) is guided vertically using the guide described in Section 3. The tape is subjected to successive application of two separate prescribed vertical loads P_0 and P_1. The initial peel arm length, l_o, or the length of tape from the initial tip position ($a = 0$) to the grip is set to 12.7 mm (0.5″) at an initial peel angle of $\theta_o = 90°$.

A load P_0 is applied at $t = 0$, with an additional weight added at $t = 3000$ s resulting in a new applied load P_1. The tape width is constant at $b_o = 48$ mm until a tip position of $a = 50$ mm (a_c) is reached, at which point the width begins to decrease linearly as a function of the tape length given in Eq. (17). Table 1 lists the values of the successively applied vertical loads (P_0 and P_1) for two experiments.

Fig. 5 shows the tip position as a function of time for the two prescribed vertical force experiments for load parameters shown in Table 1. It shows that there is a relationship between the tip position and the applied load. The instantaneous slope of the position as a function of time represents the instantaneous tip velocity. From time $t = 0$ to $t = 3000$ s, the tip velocity decreases as the time t increases for both experiments, with the tip velocity higher for a larger initial applied load P_0 (SC1). This occurs as a result of the decreasing peel angle as the crack advances (Eq. (2)).

Table 1
Applied loads, P_0 and P_1 for the prescribed vertical load (F_{perp}) experiments.

Experiment #	P_0 (N)	P_1 (N)
SC1	0.59	1.96
SC2	0.49	1.23

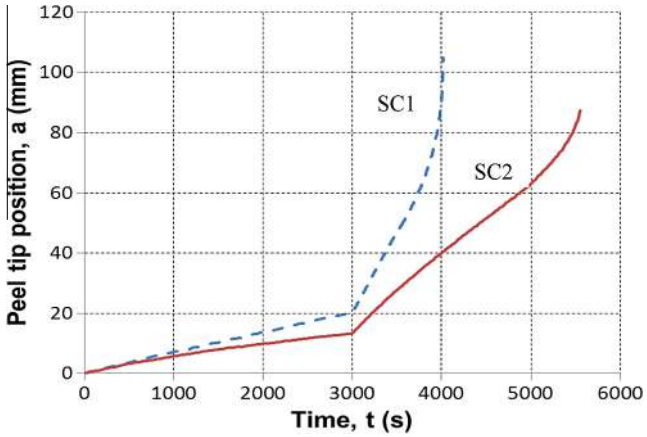

Fig. 5. Peel tip position, a, as a function of time, t, for two separate prescribed vertical force (F_{perp}) peel experiments with guided tip extremities.

Since the tip velocity is decreasing, the debonding here is stable, as it approaches an equilibrium position where it should arrest. At t = 3000 s, the weight is increased to reach a total applied load P_1, resulting in a faster tip velocity. When the load is increased to P_1, the tip velocity increases in both cases, with the peel tip in experiment #SC1 moving faster than the peel tip corresponding to experiment #SC2 as a result of the larger load. At the tip position where the width begins to decrease (a = 50 mm, $b' < 0$), the tip velocity no longer remains steady and tends towards unstable debonding. The relations in Eq. (2) and the stability criterion (Eqs. (12) and (13)) can be used to verify the point at which debonding becomes unstable in the experiment.

When $b' < 0$, it can be shown that unstable debonding occurs when the following value of the tip position is reached,

$$a^* = \frac{1}{3}\left(a_c + \frac{b_0}{|b'|} - l_0\right). \tag{18}$$

If $a^* < a_c$, the onset of unstable debonding starts when $a = a_c$

For both experiments #SC1 and #SC2, the debonding is predicted (Eq. (18)) to become unstable when the tip position reaches a^* = 52.4 mm. The correlation of this prediction with experimental results can be checked in Fig.5 where the onset of instability manifests itself by the increasing of the tip velocity of the peeling front that results in rapid peeling, which is evidenced by the inflection in the plot of peel tip position vs. time at a = 57 mm. The point of inflection is determined from abrupt change in peel front velocity, i.e., the slope of the peel tip position vs. time. It is also interesting to note that the debonding becomes unstable for the same peel tip position irrespective of the loading history (SC1, SC2), thus confirming the theoretical prediction of Eq. (11), which depends only upon geometrical parameters (a, b, l) for $K = \infty$.

4.2. Effect of stiffness (K)

4.2.1. Combined loading (F_{perp} and F_{par}) resulting in the same initial peel force, F

Experiments are conducted to investigate the effects of varying combinations of F_{perp} and F_{par0} along with varying string stiffness for tape of constant width ($b = b_o$ = 48 mm). Table 2 gives a summary of the combination of F_{perp}, F_{par0} and string widths w considered (the stiffness K is proportional to the width, Eq. (16)).

Table 2
Summary of experimental parameters for specified stiffness experiments.

Experiment#	String width, w (mm)	F_{perp} (N)	F_{par0} (N)	F_0 (N)
SK1	6.35	2.94	3.92	4.9
SK2	12.7	2.94	3.92	4.9
SK3	6.35	3.92	2.94	4.9
SK4	12.7	3.92	2.94	4.9

Note that for all combinations of F_{perp} and F_{par0}, the initial resultant peel force F_0 (Eq. (1)) is the same, F_0 = 4.9 N (500 g). The length of initial peel arm, l_0, and initial string length, L_S in all of these experiments are set to 50.8 mm (2″) and 393 mm (15.5″), respectively. A plot of the tip positions, a, of the tape as a function of time, as imaged during the experiments are shown in Fig. 6. The peeling proceeds as the string is relaxed using the stage moving at a velocity of 150 μm/s until t = 600 s and after which the stage is stopped. The corresponding outputs from the load cell for the force F_{par} as a function of time are shown in Fig. 7.

While the initial resultant force, F_0 is the same in all cases, there is a clear effect of the string stiffness, K, as well as the combination of forces F_{par0} and F_{perp}. This corresponds to the trend seen in the plot in Fig. 6. Recall from Eq. (16) that the stiffness of the string increases as the width of the string increases. Examining two curves with the same F_{perp}/F_{par0} combination but with different widths (SK1 and SK2, SK3 and SK4), the tip velocity decreases as the width of the string increases. Thus, a system with increased stiffness (K) corresponding to a larger string width results in a lower peeling rate (SK2 and SK4), i.e., more stable, which is consistent with the theoretical prediction (Eq. (10)). It is further seen from Fig. 7 that for a given F_{par0}, the decrease in F_{par} is smaller for a stiffer string over the same time increment.

It is inferred from Fig. 7 that when the stage is moving, the extremity of the tip where the weight is attached is also moving in the horizontal direction due to the advancing peel tip and the weight is not guided vertically. Since

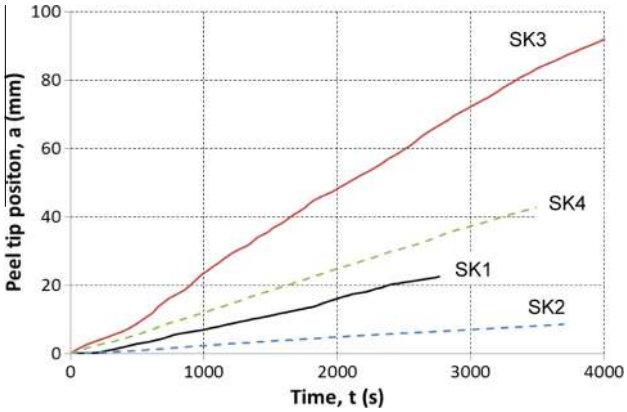

Fig. 6. Peel tip position, a as a function of time, t, for experiments with different string stiffness and combinations of F_{perp} and F_{par0} for the same initial resultant peel force F_0.

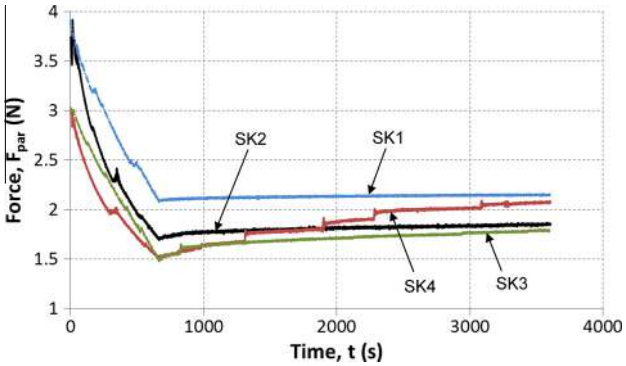

Fig. 7. Measured force parallel to the substrate, F_{par}, as a function of time, t, for experiments of variable string stiffness and various combinations of F_{perp} and F_{par0}. The corresponding tip position, a, as a function of time is shown in Fig. 6.

the tape is still debonding from the substrate after t = 600 s as is seen from the increasing tip position in Fig. 7, the parallel forceF_{par} increases even after the stage is stopped. This is a result of the tip position, a, moving away from the string while the string is fixed at the load cell resulting in the elongation of the string and thus causing a slight increase in F_{par}. The increase in F_{par} after time t = 600 s does not seem to affect the propagation of the tip velocity since the tape used here is of constant width. The experiments in Fig. 5 already show that the tip velocity increases as the applied load F_{perp} increases in the experiments where the weight is guided vertically. This is also seen in Fig. 6 by comparing experiments for the same string width (e.g., SK1 and SK3, SK2 and SK4) under increasing F_{perp}. Thus, altering the force components F_{par0} andF_{perp} has an effect on the tip velocity.

4.2.2. Varying parallel force

To examine the effect solely due to F_{par} on the tip velocity and the stability of the debonding process, experiments are conducted for a variable width tape while the stage is stopped at different amounts of time to alter the change in F_{par}. In all of these experiments, the applied load F_{perp} and initial parallel force F_{par0} are the same, 2.94 N (300 g) and 3.43 N (350 g), respectively. The same string width (w = 12.7 mm) is employed in all the experiments. In all cases, the initial length of the tape is l_o = 76.2 mm (3″). The initial tip position is set at a point in a region of the constant-width portion of the tape and 5 mm prior to reaching the variable-width portion, i.e., a_c = 5 mm. The stage stop times for the experiments are summarized in Table 3. The tip position, a, is plotted as a function of time for the four experiments with variable width tape in Fig. 8.

For all of the experiments except for a stop time of 600 s (SV4), the peel tip position when the stage is stopped is just prior to the position where the tape changes width. Fig. 8 shows that the stability of the debonding process is affected by the time at which the stage is stopped. The parallel force, F_{par} is larger for the smaller stop times. As the stop time is increased, the value ofF_{par} at the corresponding stop time is lower, resulting in an increase of the tip velocity promoting unstable peeling. While the tape debonds

Table 3
Summary of stage stop experiments with variable width tape.

Experiment#	Stage stop time (s)
SV1	300
SV2	400
SV3	500
SV4	600

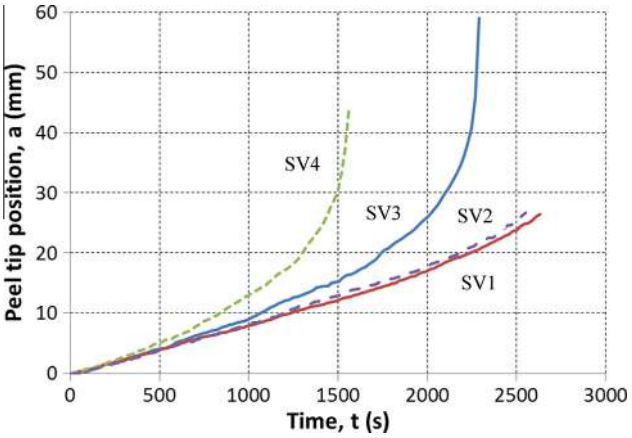

Fig. 8. Peel tip position, a, as a function of time, t, for varying stage stop times for separate experiments with tape of variable width.

completely and fails in an unstable fashion for stop times of 500 and 600 s, the tape is still attached to the substrate at the end of the experiment for the stop times of 300 and 400 s. Although the process also becomes unstable for the smaller stop times, the tip velocity increases at a slower rate. This is consistent with the theoretical stability criterion that the debonding process is unstable for the parameters considered here as suggested by Eq. (11).

4.3. Geometrically tuned instability

The tuneable position of the onset of instability can be illustrated by using a displacement-controlled peel test in which the extremity of the tape is displaced vertically at a constant rate. This corresponds to the case where the stiffness of the string in Fig. 1 is infinite, i.e., $K = \infty$ and the extremity is vertically guided. Since the displacement is controlled, the debonding process is stable. However, from this test it is possible to obtain useful information concerning the stability of debonding in a test where $K = \infty$ and F_{perp} is increased incrementally (henceforth denoted as force control experiment). The recording of the vertical component of the peel force (F_{perp}) in the displacement control experiment allows for characterizing the tip position at which F_{perp} reaches a maximum value. It can be theoretically demonstrated that this position is given by a^* (Eq. (18)) and it was shown in Section 4.1 that a^* characterizes the onset of instability in a force control test.

In Fig. 9, the vertical force F_{perp} is measured directly (from the load cell in Fig. 3) as a function of the peel tip position, a, in a displacement control test where the initial peel arm length (l_o) is 152.4 mm, the initial peel angle is $\theta_o = 90°$, the initial tip position is $a = 0$ and the tape width variation is given by Eq. (17) with $a_c = 0$. It is seen that F_{perp} decreases right after the beginning of peeling. Indeed, for the initial conditions considered here, $a^* < 0$ (Eq. (18)) and it is known that F_{perp} decreases for $a > a^*$ in a displacement control test. Thus, the theory clearly predicts that F_{perp} has to decrease right at the beginning of peeling in the test corresponding to Fig. 9. The rapid increase of F_{perp} observed in Fig. 9 at the beginning of loading corresponds just to a very short transient stage. It should be noted that,

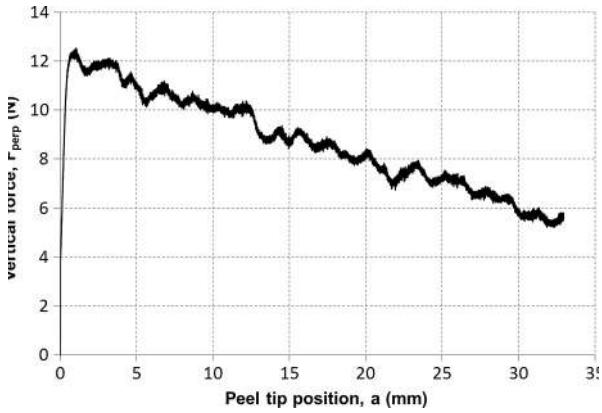

Fig. 9. Vertical component of the peel force (F_{perp}) vs. peel tip position, a, for a displacement controlled peel experiment on a variable width tape (Eq. (17)).

since $a^* < 0$, the debonding process would be initially unstable in a force control test with same initial conditions as those associated with Fig. 9.

However, for a small value of the initial peel arm, $a^* > 0$. Then, F_{perp} increases first (for $a < a^*$) in a displacement control test before reaching its maximum value at a^*. Consequently, with a small initial peel arm, the debonding process would be initially stable (the condition Eq. (12) is met) in a force control test and would become later unstable for $a > a^* > 0$.

Thus, according to the criterion in Section 2 (Eq. (11)), the geometry of the tape appears to play a direct role in determining the stability (Fig. 9). Thus, by using Eq. (11) to tune the geometry of the tape, the onset of instability can be predetermined accurately.

5. Conclusions

The stability of peeling has been examined through a series of experimental investigations aimed at understanding criteria which govern the debonding process of an inextensible adhesive tape attached to a rigid glass sub-

strate. A new experimental setup has been designed to independently vary the forces and compliance of the loading applied to the extremity of a tape adhesively bonded to a substrate. Results from an analytical model are used to understand the role of various geometrical parameters and stiffness of the loading system on the stability of peeling. The model assumes the adhesion energy to be independent of the peel velocity.

The experiments show that the stability of peeling is dependent on the stiffness of the loading system and the geometric parameters of the tape as suggested by the theoretical model. Decreasing the stiffness of the system or increasing the compliance leads to unstable peeling. The instability criteria can be cast in terms of the slope of the variation of the width of the tape and the geometrical parameters of the tape. It is demonstrated that the onset of instability is independent of the magnitude and sequence of loading and is purely dictated by the geometry of the tape. It is also shown that the onset of stability can be tuned by varying the various geometrical parameters such as the peel angle, length of the peel arm and width of the tape.

The experimental results are in general qualitative agreement with the predictions of the analytical model (Molinari and Ravichandran, 2013) but discrepancies do exist in making quantitative comparisons. These discrepancies can be attributed to the rate dependent (viscoelastic) nature of the adhesion energy on peel velocity and peel angle (Kovalchick, 2011), which changes continuously in the present peeling experiments because of the relatively short initial peel arm length. The analysis of stability becomes more complex when these effects are included. The viscoelastic nature of debonding can be seen to affect the results, stable peeling does not lead to arrest and unstable peeling does not manifest itself as abrupt or catastrophic debonding. For example, this can be observed in Fig. 5 where under the initial small vertical force (P_o), the peel front never ceases to arrest, and when subjected to a higher vertical force (P_1), the peel front upon reaching the unstable position does not lead to catastrophic debonding. Instead of arrest, the peel front decelerates continuously, and instead of abrupt debonding, the peel front accelerates rapidly.

The present study could lead to better understanding of the stability of peeling in many engineering applications, particularly where the system compliance is of importance. It could also be used to shed light on biological systems such as how a gecko alters the force magnitude and direction of the setae during attachment and detachment to maintain stability during locomotion.

Acknowledgments

CK acknowledges the support through the National Defense Science and Engineering Science Graduate (NDSEG) Fellowship. GR gratefully acknowledges the support provided by the National Science Foundation (CMMI-1201102). AM wishes to express his appreciation for the hospitality provided during his visits to Caltech.

References

Autumn, K., Dittmore, A., Santos, D., Spenko, M., Cutkosky, M.R., 2006. Frictional adhesion: a new angle on gecko attachment. J. Exp. Biol. 209, 3569–3579.

Balicki, M., Uneri, A., Iordachita, I., Handa, J., Gehlbach, P., Taylor, R., 2010. Micro-force sensing in robot assisted membrane peeling for vitreoretinal surgery. Lecture Notes in Computer Science, 6363, pp. 303–310.

Benedek, I., Feldstein, M.M. (Eds.), 2008. Applications of Pressure-sensitive Products. CRC Press, Boca Raton, FL.

Bundy, K., Schlegel, U., Rahn, B., Geret, V., Perren, S., 2000. An improved peel test method for measurement of adhesion to biomaterials. J. Mater. Sci.: Mater. Med. 11, 517–521.

Cheng, Q.H., Chen, B., Gao, H.J., Zhang, Y.W., 2011. Sliding-induced non-uniform pre-tension governs robust and reversible adhesion: a revisit of adhesion mechanisms of geckos. J. R. Soc. Interface. http://dx.doi.org/10.1098/rsif.2011.0254.

Harris, J.H., Rubel, E., 2008. The role of interfacial compound formation on package reliability. Adv. Microelectron. 35, 20–27.

Hutchinson, J.W., 1979. A Course on Non-Linear Fracture Mechanics, Lecture Notes, Department of Solid Mechanics. Technical University of Denmark, Lyngby, Denmark.

Hutchinson, J.W., Paris, P.C., 1979. Stability analysis of J-controlled crack growth in elastic-plastic fracture. In: Landes, J.D., Begley, J.A., Clarke, G.A. (Eds.), Elastic–Plastic Fracture. ASTM STP 668, American Society for Testing and Materials, Philadelphia, PA, pp. 37–64.

Kovalchick, C., 2011. Mechanics of peeling: Cohesive zone law and stability. Ph.D. Thesis, California Institute of Technology, Pasadena, CA.

Molinari, A., Ravichandran, G., 2013. Stability of peeling for systems with rate independent decohesion energy. Int. J. Solids Struct. 50, 1974–1980.

Rivlin, R.S., 1944. The effective work of adhesion. Paint Tech. 9, 215.

Tian, Y., Pesika, N., Zeng, H., Rosenberg, K., Zhao, B., McGuiggan, P., Autumn, K., Israelachivili, J., 2006. Adhesion and friction in gecko toe attachment and detachment. Proc. Nat. Acad. Sci. 103, 19320–19325.

Yao, H., Gao, H., 2006. Mechanics of robust and releasable adhesion in biology: bottom-up designed hierarchical structures of gecko. J. Mech. Phys. Solids 54, 1120–1146.